Surface resistance of cadmium in a magnetic field

V. V. Lavrova, S. V. Medvedev, V. G. Skobov, L. M. Fisher, and V. A. Yudin

A. F. Ioffe Physico-technical Institute, USSR Academy of Sciences
All-union Electrotechnical Institute

(Submitted November 20, 1972)
Zh. Eksp. Teor. Fiz. **64**, 1839-1854 (May 1973)

Doppler-shifted electron and hole cyclotron resonance and its effect on the surface resistance of cadmium in the radio-frequency range are studied theoretically and experimentally. Resistance oscillations due to excitation of electron and hole dopplerons in a plate and also impedance singularities due to the presence of thresholds in the spectrum of the waves are singled out by employing circular polarizations of the exciting field. The influence of dopplerons on the surface resistance of a bulky sample following diffuse reflection of the carriers by the surface is considered for a simple model of a paraboloid-shaped Fermi surface. It is shown that the presence of thresholds in the doppleron spectrum leads to kink in the surface resistance as a function of magnetic field strength. The field strength dependence of the impedance are in agreement with the experimental results. The electron doppleron spectrum is determined from the plate impedance oscillations, and it is indicated how the nonlocal conductivity of the metal can be determined from these data.

1. INTRODUCTION

In earlier papers[1,2] we investigated the oscillations of the surface resistance of the cadmium plate in a magnetic field perpendicular to the surface and parallel to the hexagonal axis of the crystal (observation of similar oscillations was reported also in[3]). It was shown that these oscillations are the result of excitation of electromagnetic waves (dopplerons) due to doppler-shifted cyclotron resonance (DSCR). The DSCR takes place when the length of the electromagnetic wave becomes equal to the extremal displacement of the electrons or holes during their cyclotron period. In accordance with the Kramers-Kronig relations, the resonant singularities in the absorption lead to dispersion of the dielectric constant of the electron-hole plasma of the metal, and it is this dispersion which causes the DSCR modes or dopplerons. The doppleron wavelength is close to the maximum displacement of a definite group of carriers during their cyclotron period. Therefore, when a doppleron is excited in a plate, the phase of the transmitted signal increases with increasing field, and this produces in the plates surface-resistance oscillations that are almost periodic in the field. In[1,2] we have observed and investigated dopplerons due to DSCR of electrons from the lens and holes from the monster. The oscillations connected with the excitation of the electron and hole dopplerons have significantly different periods, since the displacement of the electrons of the limiting point of the lens are approximately four times larger than the maximum displacements of the holes. The regions of existence of both waves are bounded on the side of weak magnetic fields. The threshold of the hole doppleron lies below the threshold of the electron doppleron. The results of an experimental study of both dopplerons are in good agreement with the theoretical conclusions. It follows also from the theory that the dopplerons have circular polarizations: the field of an electron doppleron rotates in the same direction as the electrons (minus polarization), and the field of the whole doppleron in the opposite direction (plus polarization). However, inasmuch as in[1,2] the waves were excited with a radio-frequency field with linear polarization, both dopplerons were observed simultaneously. Obviously, to study the doppleron it is much better to use circular polarization of the exciting field. It is such an investigation which is the subject of the present paper.

The use of circular polarization shows that the oscillations of the electron and hole dopplerons are indeed observed at different directions of the exciting-field rotation. This, first, is direct proof that the oscillations of the surface resistance of the plate are due to doppleron excitation, and not to the Gantmakher-Kaner size effect[4]. In addition, the use of circular polarizations makes it possible to investigate the singularities of the surface resistance of the bulky sample, singularities connected with the electron and hole dopplerons. The point is that the experimentally observed oscillations of the derivative of the surface impedance are observed against the background of smoother but much larger changes of dR/dH. Thus, the derivative dR/dH increases quite strongly ahead of the threshold of the electron doppleron, and oscillations are observed on the threshold section[1]. The oscillations of the hole doppleron are observed in weaker fields. These oscillations are proceded by large maximum of the derivative of resistance[2]. Unlike the doppleron oscillations, the behavior of the mentioned smooth variations of dR/dH does not depend on the thickness of the sample. This indicates that they are not connected with excitation of standing dopplerons in the plate. It is natural to assume that these stages of the derivative are singularities of the surface resistance of the bulky sample, connected with the presence of thresholds in the spectrum of the electron and hole dopplerons. Since these singularities do not have the character of oscillations and are not connected with the values of the extremal displacements of the carriers, the use of linear polarization does not make it possible to separate the effects due to electrons and holes. To the contrary, the use of circular polarizations permits separate study of the singularities of the resistance of bulk samples, due to either electron or hole dopplerons.

The influence of the wave threshold on the impedance of a metal with equal concentrations of electrons and

holes was considered by Kaner and one of the authors[5]. It was shown that in the case of specular reflection of the carriers from the surface of the metal, the impedance has a root singularity in the vicinity of the threshold. It was established later that the behavior of the impedance near the threshold depends on the character of the reflection of the carrier from the surface. In the case of the helicon threshold in an alkali metal, this was demonstrated by Alig[6]. The influence of the character of the reflection of the carriers on the impedance of a metal with equal electron and hole concentrations was considered by Azbel' and Rakhmanov[7]. They reached the conclusion that in the case of diffuse reflection, the surface resistance increases smoothly with the field, changing from a constant corresponding to the anomalous skin effect in the region of weak magnetic fields to a linear dependence corresponding to the normal skin effect in strong fields. According to Azbel' and Rakhmanov[7], in the region of the wave threshold the surface resistance has no singularities whatever in the case of diffuse reflection, and has a root singularity in specular reflection. The character of the impedance singularity observed by us near the threshold of the wave favors diffuseness of the reflection. In the present paper we consider the behavior of the surface resistance in diffuse reflection of the carriers for the model of a lens having a parabolic shape. This model was used earlier by Chambers and one of the authors[8] to study DSCR in anisotropic metals with unequal electron and hole concentrations. Although the real lens in cadmium is, of course, not parabolic, the considered model gives a qualitatively correct description of all the properties of the electron doppleron. It should also describe correctly the field dependence of the surface resistance, especially if it is recognized that the impedance singularities near the wave threshold depend not so much on the shape of the Fermi surface as on the character of the carrier reflection[6,9].

It is shown in the present paper that the surface resistance has a kink in the region of the doppleron threshold. This kink has an infinite derivative in the absence of carrier scattering, and becomes smoothed out at a finite mean free path. The derivative of the surface resistance with respect to the field therefore increases rather sharply in the vicinity of the threshold, in good agreement with experiment.

2. MEASUREMENT PROCEDURE

We measured the derivative of the surface resistance of single-crystal cadmium plates in a magnetic field perpendicular to the plane of the plate and parallel to the hexagonal axis of the crystal. The constant magnetic field was produced with a superconducting solenoid or electromagnet. The solenoid constant a = H/J was calibrated against NMR signals, and the field H was determined from the current J of the solenoid. The electromagnet field was measured with a Hall pickup calibrated with a NMR magnetometer[10] directly during the course of the measurements. A signal proportional to the magnetic field was applied to the X coordinate of an automatic potentiometer. The accuracy of the X-coordinate measurement was about 0.5%. The dc field was modulated in amplitude at a frequency 10 Hz.

The samples were plates of thickness from 0.3 to 2 mm; the normal to the plane of the sample was parallel to the [0001] axis (these samples were used earlier in[2]). The ratio of the sample resistances at 293 and 2°K, measured with direct current, was 5×10^4, so that the electron mean free path at 2°K was ~1 mm.

The pickup for the dR/dH signals was an autodyne detector with constant sensitivity[11]. The independence of the sensitivity of external factors, particularly of the magnetic field intensity, was an important characteristic of the measuring instrument, since we were interested in this study not only in the oscillations but also in the smooth dependence of the derivative of the resistance in a wide interval of magnetic fields.

The measurements were performed in a radio-frequency field having circular polarization. The polarization plane was parallel to the surface of the sample. To obtain circular polarization, the measurement setup described in[1,7] was modernized somewhat. The sample was placed in the flat inductance coil of the tank circuit of the autodyne. This coil, together with the sample, was inserted in another approximately identical coil. The coil axes made an angle 90°. A radio-frequency voltage shifted in phase by 90° with the aid of a phase shifter was applied to the external (auxiliary) coil from the autodyne detector through an amplifier. With such a coil geometry, the radio-frequency field was in the general case eliptically polarized in the plane of the sample. Since the inductances of both coils are close, the voltages on the coils should be approximately equal if circular polarization is to be obtained. These voltages were measured with a vacuum voltmeter. The voltage on the auxiliary coil was regulated by varying the gain of the amplifier. The phase shift of the voltage was monitored against Lissajoux figures on an oscilloscope. The phase was adjusted by magnetizing the ferrite core of the phase-shifter coil. The magnetization current was measured with an ammeter. The circular polarization of the radio-frequency field was set by selecting the amplitude and the phase of the voltage on the auxiliary coil. The direction of the polarization relative to the magnetic field (plus or minus polarization) was changed by interchanging the terminals of the auxiliary coil or by reversing the direction of the magnetic field.

As usual, the signal from the autodyne was detected, amplified at the modulation frequency, and fed after phase detection to the Y coordinate of the automatic potentiometer. All the measurements were made at 2°K.

3. MEASUREMENT RESULTS

Figures 1–3 show typical plots of the derivative dR/dH against the magnetic field for two circular polarizations of the exciting field. In Fig. 1 are shown plots of the resistance derivative in the region of existence of the electron doppleron in the field interval from 6 to 21 kOe. Curve 1 corresponds to minus polarization and curve 2 to plus polarization. The changeover from one polarization to the other was effected by reversing the direction of the magnetic field. Both curves were plotted at identical gains of the measurement apparatus. At the minus polarization, the plate resistance at H > 9 kOe experiences larger oscillations, due to excitation of the electron doppleron. The character of these oscillations is the same as in the case of linear polarization[1,2]. In the case of plus polarization, the oscillations of the electron doppleron are practically nonexistent: their amplitude decreases by 2 orders of magnitude.

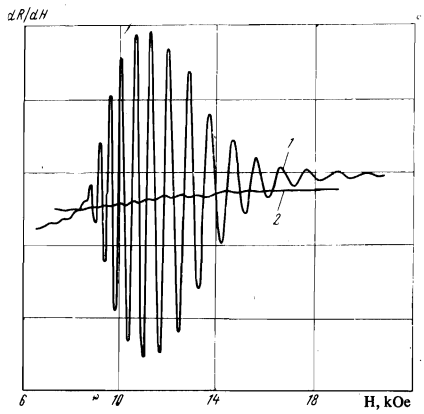

FIG. 1

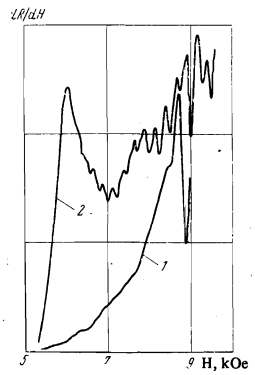

FIG. 2

FIG. 1. Plots of the oscillations of an electron doppleron in the case of circular polarization: curve 1—minus polarization, curve 2—plus polarization; frequency f = 2.68 MHz, sample thickness d = 0.57 mm, T = 2°K.

FIG. 2. Oscillations of hole dopplerons; curves 1 and 2 correspond to minus and plus polarizations, the gain for curve 1 is half that for curve 2; f = 2.68 MHz, d = 0.57 mm, T = 2°K.

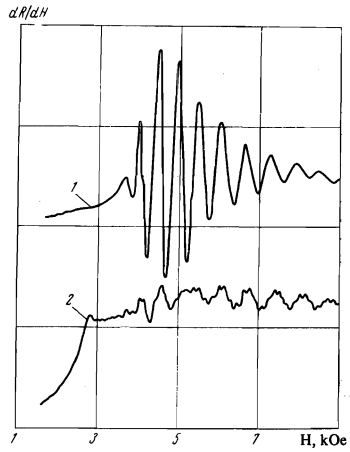

FIG. 3. Plots of the derivative of the surface resistance at 255 kHz; the gain from curve 1 (minus polarization) is 1/3 that for curve 2 (plus polarization); d = 0.57 mm, T = 2°K.

The oscillations of the hole doppleron have a smaller amplitude and cannot be observed at the given gain.

Plots of dR/dH at a larger gain, in the region of the existence of the hole doppleron, are shown in Fig. 2 (curve 1—minus polarization, curve 2—plus polarization). In the case of plus polarization, short-period oscillations are observed and are due to excitation of the hole doppleron. They are not observed in the case of minus polarization. The large-amplitude oscillations, which begin in the region of 9 kOe on curve 1, are due to the electron doppleron. The complicated picture of the oscillations on curve 2 at H > 9 kOe is connected with the presence of both hole and electron oscillations. The latter have an amplitude much smaller than that on curve 1. All the plots in Figs. 1 and 2 were obtained at f = 2.68 MHz.

The plots of the derivative of the surface resistance in the region of the existence of both the electron and the hole dopplerons at 255 kHz are shown in Fig. 3. On curve 1, corresponding to minus polarization, one can see large oscillations of the electron doppleron. On curve 2 (plus polarization) there are short-period oscillations of the hole doppleron and oscillations of the electron doppleron. The amplitude of the latter is somewhat larger than the amplitude of the hole oscillations, but much smaller than on curve 1. The presence of electron oscillations in the plus polarization on Figs. 2 and 3 is apparently due to a certain inhomogeneity of the radio-frequency field of the coils, as a result of which the polarizations were not strictly circular over the entire surface of the sample. It should be noted that the oscillations of the hole doppleron on curve 2 (Fig. 3) are present in strong fields. Observation of weak oscillations of the hole doppleron in the region of existence of large oscillations of the electron doppleron becomes possible because of the use of circular polarization and the almost complete separation of the oscillations of the two types.

Oscillations of the electron and hole doppleron are observed on relatively gently sloping sections of the $dR_{\pm}/dH$ curves. On the other hand, in the region below the threshold of the corresponding doppleron, there is a rather sharp increase of $dR_{\pm}/dH$ (see Figs. 2 and 3). For the minus polarization, this rise is monotonic, and for the plus polarization the derivative has an asymmetrical maximum, whose left slope is much larger than the right slope. At an exciting-field frequency 1 MHz, a maximum of dR_{+}/dH is observed in a field of 4.54 kOe. When the frequency is varied, all the singularities of the derivatives are shifted relative to the magnetic-field scale in proportion to the cube root of the frequency.

4. THEORY

A. Paraboloid model. The properties of the electron and hole dopplerons in cadmium were investigated theoretically earlier[1,2]. In[1] we considered the model of a spherical lens with a sharp edge, and the concentration of the holes was taken into account in a local approximation. In[2] we investigated a model closer to the real Fermi surface of cadmium, namely, we considered a lens with a rounded-off edge and took into account the DSCR of the monster holes. The models considered have led to relatively simple expressions for the nonlocal conductivity, which, however, did not make it possible to solve analytically the dispersion equation relative to the wave vector of the doppleron. The dispersion equation could be solved graphically.

In the present paper we investigate the influence of dopplerons on the peaks of a semi-infinite metal in the case of diffuse reflection of electrons from the surface. This problem can be easily solved if analytic expressions can be obtained for the roots of the dispersion equation. We consider here therefore a Fermi-surface model in which the lens consists of two cups in the form of paraboloids of revolution, and a round cylinder inserted between them. This model was used earlier to study dopplerons and their interaction with helicons in metals with non-equilibrium electron and hole densities[8].

If the magnetic field is directed along the revolution axis of the lens (hexagonal axis of the crystal), then the average displacements of all the electrons are equal on the parabolic cups, and are equal to zero on the cylindrical surface. The dimension and shape of the cups must be chosen such that the average displacement of the electrons during the cyclotron period be equal to the displacement of the electrons at the limiting point of a real lens, and the volume of the cups amount to a

specified part of the volume of the electron Fermi surface. The height of the cylindrical section is determined from the condition that a volume of the model lens is equal to the volume of the lens of real cadmium.

We choose as the hole Fermi surface two identical bodies similar to the electron lens, but of smaller dimensions. The concentrations of the electrons and holes in cadmium are equal, and the maximum displacement of the monster holes during the cyclotron period is one quarter the displacement of the electrons of the limiting point of the lens. These conditions, together with specification of the fraction of carriers situated inside the parabolic cups, determine completely the shape and dimensions of the Fermi surface. It remains for us to determine the parameters α_1 and α_2 that characterize the fractions of the electrons and holes inside the parabolic cups. We choose these parameters such that the values of the threshold fields for the electron and hole dopplerons coincide with the values observed in experiment.

The model of paraboloidal Fermi surface is convenient because the carriers on the surfaces of the paraboloids have identical average displacements along the field and participate simultaneously in the DSCR. Resonance set in when the length of the electromagnetic wave becomes equal to the displacement of these carriers during the cyclotron period. These carriers lead to singularities of the pole type in the nonlocal conductivity. On the other hand, the carriers on the cylindrical surfaces have no displacements along the field and make a purely local contribution to the conductivity. It should be noted, however, that the constancy of the carrier displacement on the paraboloid surface, which makes this model simple and attractive, leads at the same time to an essential fundamental shortcoming in that there is no collisionless cyclotron absorption in the region where the length of the electromagnetic wave is smaller than the carrier displacement:

$$ku_j/2\pi > 1. \tag{1}$$

Here k is the wave vector, u_j is the displacement of the carriers of type j,

$$u_j = 2\pi c p_j / e_j H, \quad j = 1, 2, \tag{2}$$

the subscript 1 pertains to electrons, the subscript 2 to holes, e_j is the carrier charge, p_j are parameters with the dimension of momentum and determine the curvature of the electron and hole paraboloids, c is the speed of light, and H is the magnetic field intensity.

In the case of real Fermi surfaces there exists in the region (1) collisionless cyclotron absorption that causes the wave to become damped. In our model, on the other hand, we obtain dispersion-equation solutions that describe weakly-damped dopplerons with wave numbers $k \gtrsim 2\pi/u_j$. Thus, a hole doppleron with wave vector $k > 2\pi/u_2$ is produced in minus polarization and an electron doppleron with wave vector $k > 2\pi/u_1$ in plus polarization. The wavelengths of these dopplerons lie in a region where there should exist a strong cyclotron absorption of the waves by the corresponding carriers. The absence of this damping and the appearance of additional weakly damped waves is a shortcoming of our model. We shall investigate the influence of the dopplerons on the field dependence of surface resistance in the case of diffuse reflection of the carriers. It will be seen from the analysis that follows that the singularities of the resistance as functions of H depend not so much on the details of the doppleron dispersion law as on the presence of a threshold near which the character of the solution of the dispersion equation changes abruptly. The dispersion-curve section near the threshold is adequately described by our model, and as a result we obtain a correct description of the surface resistance.

B. Nonlocal conductivity. The dispersion equation for a circular-polarization wave propagating along the magnetic field H (the z axis) is given by

$$k^2c^2 = 4\pi i\omega\sigma_\pm(k, H), \tag{3}$$

where

$$\sigma_\pm = \sigma_{xx} \pm i\sigma_{yx}, \tag{4}$$

σ_{xx} and σ_{yx} are elements of the tensor of nonlocal conductivity in the transverse plane. It is obvious that $\sigma_\pm$ is the sum of the contributions of the electrons and holes:

$$\sigma_\pm = \sigma_\pm^{(1)} + \sigma_\pm^{(2)}. \tag{5}$$

In the case of a Fermi surface in the form of a paraboloid, the expression for the nonlocal conductivity can be written in the form[8]

$$\sigma_\pm^{(j)}(k, H) = -i\frac{Ne_jc}{H}\left\{\frac{\alpha_j/2}{\pm 1 - i\gamma_j - ku_j/2\pi} + \frac{\alpha_j/2}{\pm 1 - i\gamma_j + ku_j/2\pi} + \frac{1-\alpha_j}{\pm 1 - i\gamma_j}\right\}, \tag{6}$$

where

$$\gamma_j = cm_j\nu_j/e_jH, \quad e_1 = -e_2 = -e, \tag{7}$$

N is the concentration of the electrons and holes, m_j is the cyclotron mass of the carriers of a given type, ν_j is the frequency of the collisions with the lattice, the expression for the displacement of the resonant carriers e_j is determined by formula (2), and α_1 and α_2 are the relative fractions of the resonant electrons and holes, respectively. The first term in the curly brackets of (6) describes the nonlocal conductivity of the resonant carriers moving in opposition to the wave. The second term corresponds to carriers moving in the same direction as the wave. The third term represents the local contribution from nonresonant carriers on the cylindrical surface.

Using formula (6), we can easily reduce the expression for the total conductivity to the form

$$\sigma_-(k, H) = \sigma_+(k, -H) = -i\frac{Nec}{H}\left\{\frac{\alpha_1k^2}{(\varkappa_1^2 - k^2)(1 + i\gamma_1)} - \frac{\alpha_2k^2}{(\varkappa_2^2 - k^2)(1 + i\gamma_2)} + \frac{1}{1 + i\gamma_1} - \frac{1}{1 + i\gamma_2}\right\}, \tag{8}$$

where

$$\varkappa_j = \frac{2\pi}{u_j}(1 + i\gamma_j) = \frac{e_jH}{p_jc} + \frac{i}{l_j}, \quad l_j = \frac{p_j}{m_j\nu_j}, \tag{9}$$

$l_{1,2}$ are the electron and hole mean-free paths.

For simplicity we confine ourselves in the analysis that follows to the case when the ratio of the collision frequency to the cyclotron frequency is the same for the electrons and holes:

$$\gamma_2 = -\gamma_1 = \gamma, \tag{10}$$

and assume that the strong-field approximation is satisfied, namely

$$\gamma \ll 1. \tag{11}$$

C. Solution of dispersion equations for minus polarization. To obtain the dispersion equation it suffices to substitute (8) in (3), which yields

$$\left\{\frac{\alpha_1}{(\varkappa_1^2-k^2)(1-i\gamma)}-\frac{\alpha_2}{(\varkappa_2^2-k^2)(1+i\gamma)}+\frac{2i\gamma}{k^2}\right\}k_H^2=1, \tag{12}$$

$$k_H^2=4\pi\omega Ne/cH, \tag{13}$$

where k_H is the wave vector of a helicon in a metal with one type of carrier in the local limit.

The dispersion equation (12) is bicubic relative to the wave vector k. We are interested in those three solutions whose imaginary parts are positive. To find them we can use the fact that they have essentially different values. We seek the solutions of the dispersion equation in the region of not very weak fields, where

$$k_H^2 \ll \varkappa_2^2. \tag{14}$$

The value of one of the roots exceeds $\varkappa_2$. To obtain an approximate value of this root it suffices to retain only the second term in the left-hand side of (12). This yields

$$k_2 \approx \varkappa_2 + \alpha_2 k_H^2/2\varkappa_2. \tag{15}$$

The two other roots do not exceed $|\varkappa_1|$ and turn out to be small in comparison with k_2. To obtain an equation that determines these roots we can therefore neglect the term k^2 in comparison with $\varkappa_2^2$ in the denominator of the second term of the left-hand side of (12). It is convenient to rewrite the obtained equations in the form

$$\xi\left\{\frac{1}{1-k^2/\varkappa_1^2}+2i\gamma\frac{\varkappa_1^2}{\alpha_1 k^2}\right\}=1, \tag{16}$$

where

$$\xi=\alpha_1 k_H^2\varkappa_2^2/k_2^2\varkappa_1^2(1-i\gamma). \tag{17}$$

The roots of (16), which are of interest to us, are given by

$$k_{0,1}=\mp\varkappa_1\left\{\frac{1}{2}\left(1-\xi+\frac{2i\gamma}{\alpha_1}\xi\right)\mp\left[\frac{1}{4}\left(1-\xi+\frac{2i\gamma}{\alpha_1}\xi\right)^2-\frac{2i\gamma}{\alpha_1}\xi\right]^{1/2}\right\}^{1/2}. \tag{18}$$

In the limit of an infinite carrier mean free path ($\gamma \to 0$), the root k_0 vanishes and k_1 takes the form

$$k_1^{(0)}=-\frac{eH}{p_1 c}[1-\xi_0]^{1/2}, \tag{19}$$

where ξ_0 is the value of ξ at $\gamma = 0$.

Let us discuss the physical meaning of the obtained solutions. The root k_2, the value of which exceeds $\varkappa_2$, is connected with the DSCR of the holes and describes a hole doppleron. As already noted above, the existence of the doppleron with wave number $k > \varkappa_2$ is the consequence of our model, in which there is no cyclotron absorption in this region. In a real metal, the root k_2 would be complex and the hole doppleron with minus polarization would be damped.

The root k_1 is due to DSCR of the lens electrons and describes an electron doppleron. It follows from (19) that in the collisionless limit $k_1^{(0)}$ is real when $\xi_0 < 1$ and imaginary when $\xi_0 > 1$. This means that the electron doppleron has a threshold at a magnetic-field value corresponding to the conditions

$$\xi_0 = 1. \tag{20}$$

If we neglect the insignificant difference between k_2^2 and $\varkappa_2^2$, then we can represent ξ approximately in the form

$$\xi \approx \frac{\omega}{\omega_L}(1-i\gamma)^{-3}, \quad \omega_L=\frac{eH^3p_1^2}{4\pi\alpha_1 Nc}, \tag{21}$$

where the quantity ω_L, which is proportional to the cube of the magnetic field, has the meaning of the limiting frequency of the electron doppleron. Expression (19) for $k^{(0)}$ takes the form

$$k_1^{(0)}=-\frac{eH}{p_1 c}\left[1-\frac{\omega}{\omega_L}\right]^{1/2}. \tag{22}$$

With increasing field, the quantity (22) increases from zero value at $\omega_L = \omega$ and approaches the limiting value $-eH/p_1c$.

The dependence of $k_1^{(0)}$ on the magnetic field H is shown in Fig. 4 (curves 3 and 3′) for the parameter values

$$N=5\cdot10^{21}\ \text{cm}^{-3},\quad p_1=1.5\hbar\text{Å}^{-1},\quad p_2=p_1/4,\quad \alpha_1=0.4,\quad \alpha_2=0.8 \tag{23}$$

and the frequency f = 3 MHz. The solid curve 3 lies above the threshold and corresponds to a real value of $k^{(0)}$. The dashed curve 3′ is below the doppleron threshold and corresponds to the imaginary value of $k_1^{(0)}$.

Carrier scattering leads to the appearance of an imaginary part of k_1, describing the damping of the electron doppleron, and also to the appearance of a complex root k_0. In the region of strong fields, the asymptotic expressions for k_1 and k_0 are

$$k_1=\varkappa_1(1-\xi)^{1/2}, \tag{24}$$

$$k_0 \approx (2i\gamma k_H^2)^{1/2}=(1+i)(4\pi Nmv\omega)^{1/2}/H. \tag{25}$$

The root k_0 describes the normal skin effect in a magnetic field, and the depth of the skin layer is proportional to H. Plots of the real (curves 0 and 1) and imaginary (curves 0′ and 1′) part of k_0 and k_1 at l_1 = 1 mm are shown in Fig. 4.

D. Solution of the dispersion equation for plus polarization. We consider now the properties of the hole doppleron. Substituting the expression for $\sigma_+(k, H)$ in (3), we obtain the dispersion equation

$$\left\{-\frac{\alpha_1}{(\bar{\varkappa}_1^2-k^2)(1+i\gamma)}+\frac{\alpha_2}{(\bar{\varkappa}_2^2-k^2)(1-i\gamma)}+\frac{2i\gamma}{k^2}\right\}k_H^2=1, \tag{26}$$

$$\bar{\varkappa}_j(H)=\varkappa_j(-H). \tag{27}$$

The roots of the equations will be designated K_S.

We separate first the smallest root K_0. Neglecting the term k^2 in comparison with $\varkappa_1^2$ in the first term of

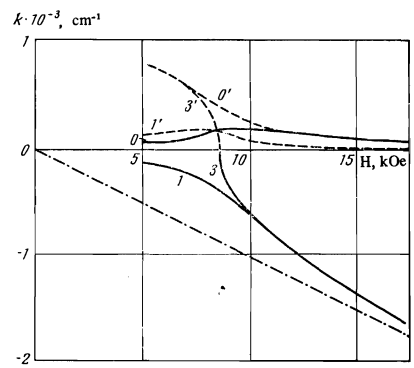

FIG. 4. Solutions of the dispersion equation for minus polarization. The solid curves 0 and 1 show the real part of the roots k_0 and k_1 at l_1 = 1 mm, and the dashed curves 0′ and 1′ the imaginary parts; curves 3 and 3′ show the real and imaginary parts of k_1 in the collisionless limit, f = 3 MHz.

(26) omitting the second term in the left-hand side of (26), we get

$$K_0 \approx (1+i)[(1+\xi^*)\gamma k_H^2]^{1/3}. \quad (28)$$

The equation for the two remaining roots takes the form

$$-\frac{\alpha_1 k_H^2}{(\bar{\varkappa}_1^2 - k^2)(1+i\gamma)}\left(1+\frac{K_0^2}{\bar{\varkappa}_1^2}\right)+\frac{\alpha_2 k_H^2}{(\bar{\varkappa}_2^2 - k^2)(1-i\gamma)}\left(1+\frac{K_0^2}{\bar{\varkappa}_2^2}\right)=1, \quad (29)$$

and its solutions are given by

$$K_{1,2} = \mp\left\{\frac{1}{2}\left[\bar{\varkappa}_1^2+\bar{\varkappa}_2^2+\frac{\alpha_1 k_H^2}{1+i\gamma}\left(1+\frac{K_0^2}{\bar{\varkappa}_1^2}\right)-\frac{\alpha_2 k_H^2}{1-i\gamma}\left(1+\frac{K_0^2}{\bar{\varkappa}_2^2}\right)\right]\right.$$
$$\pm\left[\frac{1}{4}\left(\bar{\varkappa}_2^2-\bar{\varkappa}_1^2-\frac{\alpha_1 k_H^2}{1+i\gamma}\left(1+\frac{K_0^2}{\bar{\varkappa}_1^2}\right)-\frac{\alpha_2 k_H^2}{1-i\gamma}\left(1+\frac{K_0^2}{\bar{\varkappa}_2^2}\right)\right)^2\right. \quad (30)$$
$$\left.\left.-4\alpha_1\alpha_2 k_H^4\left(1+\frac{K_0^2}{\bar{\varkappa}_1^2}\right)\left(1+\frac{K_0^2}{\bar{\varkappa}_2^2}\right)\right]^{1/2}\right\}^{1/2}.$$

In the region of strong fields ($\xi \ll 1$), the root K_0 is asymptotically equal to k_0 determined by formula (25), and the expressions for K_1 and K_2 become

$$K_1 = [\bar{\varkappa}_1^2 + \alpha_1 k_H^2]^{1/3}, \quad K_2 = -[\bar{\varkappa}_2^2 - \alpha_2 k_H^2]^{1/3}. \quad (31)$$

The root K_1 is connected with electron DSCR and describes an electron doppleron in plus polarization. This root is somewhat larger than $\bar{\varkappa}_1$, i.e., it is located in a region where strong cyclotron absorption of the wave by the lens electrons should take place. The existence of a weakly damped electron doppleron in plus polarization is a consequence of our model. In a real metal, such a wave should be damped.

The root K_2 is connected with DSCR of the holes and describes a hole doppleron. It is located in the region $k < \bar{\varkappa}_2$ where there is no hole cyclotron absorption, but there is electron cyclotron absorption. The magnitude of the latter, however, decreases rapidly with increasing $k - \bar{\varkappa}_1$, and is small at $k \lesssim \bar{\varkappa}_2$. Therefore the hole doppleron in plus polarization is weakly damped. With decreasing magnetic field, the value of K_1^2 increases while K_2^2 decreases, so that they become equal at a certain value of H. This is the location of the doppleron threshold. Plots of the real (curves 1 and 2) and imaginary (curves 1′ and 2′) parts of K_1 and K_2 in the vicinity of the threshold are shown in Fig. 5. These curves have kinks at $H \approx 6.6$ kOe; curves 1′ and 2′, which describe doppleron damping, decrease in strong fields and increase sharply in weak fields. At $H < 6.6$ kOe, the damping becomes large and the wave cannot propagate. Curve 0 on Fig. 5 shows the real part of the root K_0, which coincides with its imaginary part. This root corresponds to the electromagnetic-field component describing the normal skin effect in a magnetic field.

E. Surface resistance. Let us examine the influence of dopplerons on the magnetic-field dependence of the surface resistance of a semi-infinite metal. Since most carriers in a metal are reflected diffusely from the surface, we confine ourselves to pure diffuse reflection. In this case the surface impedance is determined by the general expression[12]

$$Z_\pm(\omega, H) = R_\pm - iX_\pm = 4\pi\omega / c^2 I_\pm(\omega, H) \quad (32)$$

where

$$I_\pm(\omega, H) = \frac{i}{\pi}\int_0^\infty dk \ln\left[1 - \frac{4\pi i\omega\sigma_\pm(k, H)}{k^2c^2}\right], \quad (33)$$

R and X are the real and imaginary parts of the impedance.

If we substitute formula (8) for the nonlocal conductivity in (33) and factorize the argument of the logarithm, then I_- takes the form

$$I_- = \frac{i}{\pi}\int_0^\infty dk \ln\frac{(k^2-k_0^2)(k^2-k_1^2)(k^2-k_2^2)}{k^2(k^2-\varkappa_1^2)(k^2-\varkappa_2^2)}. \quad (34)$$

The function I_+ is determined by an integral obtained from (34) with the aid of the substitution

$$k_0 \to K_0, \quad k_j \to K_j, \quad \varkappa_j \to \bar{\varkappa}_j, \quad (j=1, 2). \quad (35)$$

The explicit form of I_- can be easily obtained by using the formula

$$i\int_0^\infty dk \ln\frac{k^2-a_1^2}{k^2-a_2^2} = \pi(a_1 - a_2), \quad \operatorname{Im} a_{1,2} > 0. \quad (36)$$

As a result we find that the surface resistance for minus polarization is given by

$$R_-(H) = \frac{4\pi\omega}{c^2}\operatorname{Re}\frac{1}{k_0 + k_1 + k_2 - \varkappa_1 - \varkappa_2}, \quad (37)$$

and R_+ is obtained from (37) by means of the substitution (35).

In the collisionless limit, the resistance R_- can be expressed in the form

$$R_-^{(0)} = \frac{4\pi\omega p_1}{ceH}\operatorname{Re}\left[1-\left(1-\frac{\omega}{\omega_L}\right)^{1/2}+\frac{1}{4}\frac{\omega}{\omega_L}\right]^{-1}, \quad (38)$$

where we have used the fact that above the threshold of the electron doppleron we have

$$k_2 - \varkappa_2 \approx \frac{\alpha_2}{8\alpha_1}\frac{\omega}{\omega_L}\varkappa_1. \quad (39)$$

It is seen from (38) that at $\omega_L = \omega$ the surface resistance has a kink due to the existence of a doppleron threshold. In the collisionless limit, the kink has an infinite derivative.

A plot of $R_-^{(0)}(H)$ at f = 3 is shown in Fig. 6 (curve 3). The carrier-lattice collisions smooth out the peak. The

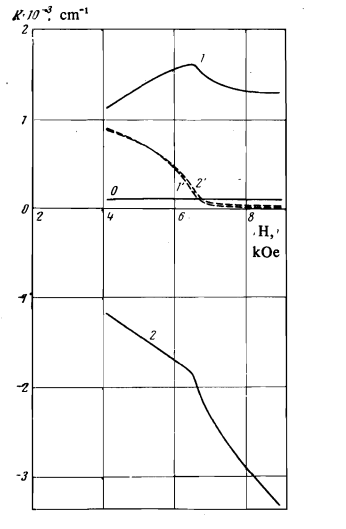

FIG. 5

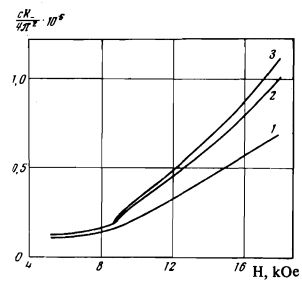

FIG. 6

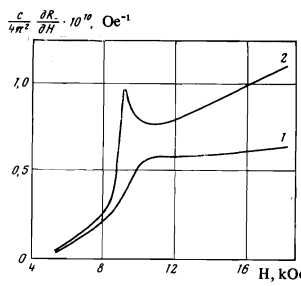

FIG. 7

FIG. 5. Plots of the real parts (curves 0–2) and of the imaginary parts (curves 1′ and 2′) of the roots of the dispersion equation for plus polarization, f = 3 MHz, l_1 = 1 mm, l_2 = 0.25 mm.

FIG. 6. Plots of the surface resistance for minus polarization at f = 3 MHz; curve 1 corresponds to the electron mean free path l_1 = 1 mm, curve 2–l_1 = 2 cm, curve 3–$l_1 = \infty$.

FIG. 7. Plots of the derivative dR_-/dH for l_1 = 1 mm (curve 1) and l_1 = 2 cm (curve 2), f = 3 MHz.

values of $R_-(H)$ for $l_1 = 1$ mm and $l_2 = 2$ cm are represented respectively by curves 1 and 2. We see that in spite of the smoothing of the kink the general character of the behavior of R_- near the doppleron threshold remains the same, namely, R_- varies with H slowly below the threshold, and more rapidly above the threshold. The slope of the plot of R_- in the region $\omega_L > \omega$ depends on the electron mean free path. The singularities of the behavior of the resistance R_- near the threshold are seen more clearly in Fig. 7, which shows the derivative dR_-/dH. Curves 1 and 2 correspond to an electron mean free path 1 mm and 2 cm, respectively. At the larger mean free path ($l_1 = 2$ cm) the derivative of the resistance has a sharp maximum in the vicinity of the threshold, and in the region of stronger magnetic fields it increases uniformly. At the smaller mean free path (curve 1), the plot of dR_-/dH takes the form of a smeared-out step.

The field dependence of the surface resistance for plus polarization can be obtained in similar fashion. Plots of $R_+(H)$ and dR_+/dH in the vicinity of the hole-doppleron threshold are shown for $l_1 = 1$ mm in Fig. 8. The behavior of R_+ near the threshold of the hole doppleron is analogous to the behavior of R_- near the threshold of the electron doppleron. The derivative dR_+/dH has an asymmetrical maximum with a steep and long left-hand slope and with a more gently-sloping and shorter right-hand slope. In strong fields, the function dR_+/dH increases slowly with H.

We have considered above only the real part of the surface impedance of a semi-infinite metal. We are unable to obtain the correct order of magnitude of the imaginary part. The point is that in our model the absence of cyclotron absorption in the hole doppleron greatly increases its damping near the threshold. Therefore X_+ turns out to be smaller in our model than in a real metal, where the lens electrons produce cyclotron damping of the hole doppleron.

5. DISCUSSION OF RESULTS

We proceed now to a discussion and comparison of the experimental and theoretical results. We must note first that the use of circular polarization of the exciting field has made it possible to determine experimentally the polarization of the oscillations of the plate impedance. The fact that the short-period oscillations are present only in the case of plus polarization and the long-period in the case of minus polarization (see Figs. 1–3) proves directly that they are due to excitation of weakly-damped electromagnetic waves, and are not connected with the radial-frequency size effect in the normal field[4]. The point is that the size effect is due to the presence of branch points in the nonlocal conductivity σ as a function of k. These branch points are present both in $\sigma_+(k)$ and in $\sigma_-(k)$, and therefore the amplitude of the size effect depends little on the polarization of the exciting field. The situation is different with doppleron waves, which are natural oscillations of an electron-hole plasma and have a definite circular polarization. Thus, separation of the electron and hole oscillations when circular polarization is used is direct proof that the observed oscillations are connected with doppleron excitation.

The second result obtained with the aid of circular polarizations is the separation of the singularities of the surface resistance of a bulk sample, due to the presence of thresholds for the electron and hole dopplerons. It is seen from Fig. 3 that doppleron oscillations of both types are observed against a relatively slowly varying background of the derivatives $dR_\pm/dH$. The onset of the oscillations is preceeded by sections of rather sharp rises in these derivatives. As follows from the theory, these rises are due to kinks of the functions $R_\pm/H$ in the vicinities of the hole and electron doppleron thresholds, respectively. At a large electron mean free path ($l_1 = 2$ cm), the derivative dR_-/dH has an asymmetrical maximum (curve 2 on Fig. 7). Inasmuch as the electron mean free path in the investigated cadmium samples was apparently on the order of 1 mm, the derivative dR_-/dH should take the form of a step. Comparison of curve 1 of Fig. 7 with curve 1 of Fig. 3 shows good agreement between the results of the theory and experiment.

Qualitative agreement between the experimental and theoretical curves is obtained also for plus polarization (compare curve 2 of Fig. 8 with curve 2 of Fig. 3). The maximum of dR_+/dH on the experimental curve of Fig. 3 is more asymmetrical than the maximum on the theoretical curves. This is apparently due to the fact that in our model there is no cyclotron damping for the hole doppleron. Cyclotron absorption of the wave by the lens electrons should increase the damping of the hole doppleron near the threshold and split up the maximum of dR_+/dH, i.e., should make the curves more similar in shape to a smeared-out step.

In conclusion let us discuss the connection of the plate-resistance oscillations with the doppleron spectrum and with the nonlocal conductivity $\sigma(k, H)$. The field of a doppleron wave passing through a plate of thickness d contains a phase factor $\exp[ik(H)d]$, the variation of which with the field is indeed the cause of the resistance oscillations. In strong fields, the wave number of the electron doppleron tends to $-eH/p_1c$, so that the oscillations become periodic. The limiting value of the period is

$$\Delta H_L = 2\pi c p_1 / ed. \tag{40}$$

Let H_S be the magnetic field corresponding to one of the last distinguishable maxima of dR_-/dH. Dividing H_S by ΔH_L, we can obtain the number s of wavelenths spanned by the thickness of the sample at a given value of the field:

$$H_s / \Delta H_L = s + {}^1/_2; \tag{41}$$

the term 1/2 in the right-hand side is connected with the antisymmetrical character of plate excitation. Determining in this manner the number of the given maximum, we can ascribe numbers to all the maxima on the experimental curves. It suffices to determine the spec-

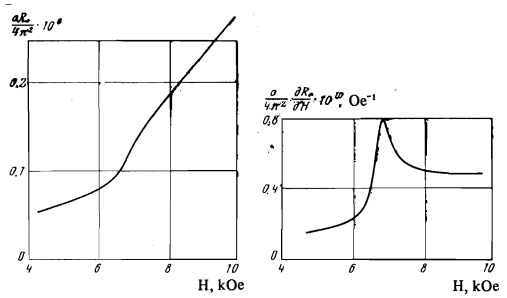

FIG. 8. Plots of $R_+(H)$ and dR_+/dH at 3 MHz, $l_1 = 1$ mm, $l_2 = 0.25$ mm.

trum of the doppleron in a number of discrete points:

$$k(H_n)=\frac{2\pi}{d}\left(n+\frac{1}{2}\right), \qquad n=1,2,\ldots s, \tag{42}$$

where n is the number of the maximum and H_n is the corresponding value of the magnetic field.

Figure 9 shows plots of the function k(H) for two different models of the lens, as well as the experimental points $k(H_n)$. The theoretical curve 1 corresponds to the paraboloidal model, and curve 2 corresponds to the model of a lens with rounded-off edge, which was considered in[2] (variant with quadratic dependence of the derivative of the cross section area $\partial S/\partial p_z$ on p_z). The error of the experimental points, due mainly to the error in the determination of the sample thickness, is ~2%. We see that the experimental points lie close to curve 2. Curve 1 shows a larger deviation, but qualitatively it describes correctly the electron-doppleron spectrum.

Knowledge of the k(H) dependence makes it possible to determine the nonlocal conductivity $\sigma(k, H)$. It was shown in[2] that the conductivity $\sigma_-(k, H)$ can be written in the form

$$\sigma_-(k,H)=-i\frac{ec}{H}\left\{\frac{1}{1+i\gamma_1}F_1\left(\frac{k}{\varkappa_1}\right)-\frac{1}{1+i\gamma_2}F_2\left(\frac{k}{\varkappa_2}\right)\right\}. \tag{43}$$

The function F_1 and F_2 describe nonlocal effects in the conductivity: in the local limit as $k \to 0$, they are equal to the carrier density N. The explicit form of these functions is determined by the conduction-electron dispersion law. Substituting (43) in (3) and neglecting small terms of order $i\gamma_j$, we obtain the equation

$$F_1(q)-F_2\left(q\frac{p_2}{p_1}\right)=\frac{k^2cH}{4\pi\omega e}, \tag{44}$$

$$q=-kcp_1/eH. \tag{45}$$

The use of relation (42) enables us to find the difference $F_1 - F_2$ for a number of the three values of the argument q:

$$F_1(q_n)-F_2\left(\frac{q_np_2}{p_1}\right)=\frac{\pi cH_n}{\omega ed^2}\left(n+\frac{1}{2}\right)^2, \tag{46}$$

where

$$q_n=\frac{cp_1k(H_n)}{eH_n}=\frac{\Delta H_L}{H_n}\left(n+\frac{1}{2}\right). \tag{47}$$

We have expressed q_n in terms of the limiting value of the period of the doppleron oscillations, using the connection of p_1 with ΔH_L(40).

It should be noted that since the period of the doppleron oscillations is $\Delta H \ll H_L$[1], the values of q_n in (47) turn out to be automatically smaller than unity. There is therefore no cyclotron absorption and the function F_1 and F_2 are real. From the values of $F_1 - F_2$ at the points q_n we can plot this difference as a function of continuous q. According to (43), however, the difference $F_1 - F_3$ differs from $\sigma_-(k, H)$ only by a factor $-iec/H$. Thus, the nonlocal conductivity of a metal can be determined in principle from the doppleron oscillations of the plate resistance.

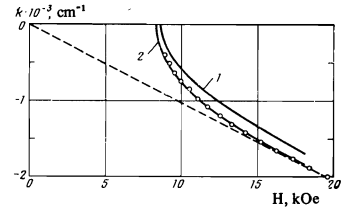

FIG. 9. Spectrum of electron doppleron at f = 3 MHz. Curve 1 corresponds to the paraboloidal model, curve 2 corresponds to the model of a lens with rounded-off edge considered in [2] (n = 2); the points correspond to the experimental results (the theoretical curves were plotted for the value $p_1/h = 1.48\text{Å}^{-1}$).

The authors are grateful to V. G. Fastovskiĭ for interest in the work and to A. V. Gavrilov for technical help.

[1] L. M. Fisher, V. V. Lavrova, V. A. Yudin, O. V. Konstantinov, and V. G. Skobov, Zh. Eksp. Teor. Fiz. 60, 759 (1971) [Sov. Phys.-JETP 33, 410 (1971)].
[2] O. V. Konstantinov, V. G. Skobov, V. V. Lavrova, L. M. Fisher, and V. A. Yudin, Zh. Eksp. Teor. Fiz. 63, 224 (1972) [Sov. Phys.-JETP 36, 118 (1973)].
[3] V. P. Naberezhnykh and L. T. Tsimbal, Sol. St. Comm., 9, 693 (1971).
[4] V. F. Gantmakher and É. A. Kaner, Zh. Eksp. Teor. Fiz. 48, 1571 (1965) [Sov. Phys.-JETP 21, 1053 (1965)].
[5] E. A. Kaner and V. G. Skobov, Phys. Lett., 25A, 105 (1967).
[6] R. Alig, Phys. Rev., 165, 833 (1968).
[7] M. Ya. Azbel' and S. Ya. Rakhmanov, Zh. Eksp. Teor. Fiz. 57, 295 (1969) [Sov. Phys.-JETP 30, 163 (1970)].
[8] R. G. Chambers and V. G. Skobov, J. Phys., F1, 202 (1971).
[9] D. S. Falk, B. Gerson, and J. F. Carolan, Phys. Rev., B1, 407 (1970).
[10] V. A. Yudin, Prib. Tekh. Eksp. No. 6, 188 (1967).
[11] V. A. Yudin and L. M. Fisher, Prib. Tekh. Eksp. No. 3, 131 (1971).
[12] G. E. Reuter and E. H. Sondheimer, Proc. Roy. Soc., A195, 336 (1948).

Translated by J. G. Adashko
197